Reduced immunopathology and mortality despite tissue persistence in a *Mycobacterium tuberculosis* mutant lacking alternative σ factor, SigH

Deepak Kaushal*, Benjamin G. Schroeder†, Sandeep Tyagi*, Tetsuyuki Yoshimatsu*, Cherise Scott*, Chiew Ko*, Liane Carpenter†, Jyoti Mehrotra*, Yukari C. Manabe*, Robert D. Fleischmann†, and William R. Bishai*‡

*Department of Medicine, Center for Tuberculosis Research, Johns Hopkins School of Medicine, 424 North Bond Street, Baltimore, MD 21231; and †The Institute for Genomic Research, 9712 Medical Center Drive, Rockville, MD 20850

Edited by Barry R. Bloom, Harvard School of Public Health, Boston, MA, and approved March 29, 2002 (received for review January 30, 2002)

The pathogenesis of tuberculosis involves multiple phases and is believed to involve both a carefully deployed series of adaptive bacterial virulence factors and inappropriate host immune responses that lead to tissue damage. A defined *Mycobacterium tuberculosis* mutant strain lacking the *sigH*-encoded transcription factor showed a distinctive infection phenotype. In resistant C57BL/6 mice, the mutant achieved high bacterial counts in lung and spleen that persisted in tissues in a pattern identical to those of wild-type bacteria. Despite a high bacterial burden, the mutant produced a blunted, delayed pulmonary inflammatory response, and recruited fewer $CD4^+$ and $CD8^+$ T cells to the lung in the early stages of infection. In susceptible C3H mice, the mutant again showed diminished immunopathology and was nonlethal at over 170 days after intravenous infection, in contrast to isogenic wild-type bacilli, which killed with a median time to death of 52 days. Complete genomic microarray analysis revealed that *M. tuberculosis sigH* may mediate the transcription of at least 31 genes directly and that it modulates the expression of about 150 others; the SigH regulon governs thioredoxin recycling and may be involved in the maintenance of intrabacterial reducing capacity. These data show that the *M. tuberculosis sigH* gene is dispensable for bacterial growth and survival within the host, but is required for the production of immunopathology and lethality. This phenotype demonstrates that beyond an ability to grow and persist within the host, *M. tuberculosis* has distinct virulence mechanisms that elicit deleterious host responses and progressive pulmonary disease.

Tuberculosis is one of the leading infectious causes of death and claims ≈2 million lives annually (1). There is controversy over whether the disease is primarily a dysfunctional immunologic reaction to a persistent microbe or whether the bacteria themselves produce tissue damage; there is evidence that both host and bacterial factors play key roles in disease severity. In susceptible mouse strains, such as C3H, the pathogen elicits a dysregulated, necrotizing host immune response leading to tissue destruction and further bacterial replication. In resistant mice such as C57BL/6, *Mycobacterium tuberculosis* survives in high numbers for many months and is contained in organized granulomatous lesions in the lung without progressive lung damage. Thus whereas mycobacteria survive in both genetic backgrounds, disease progression is delayed in resistant animals (2–4).

On the bacterial side, *M. tuberculosis* virulence has been associated with its initial survival within macrophages and resistance to reactive oxygen and nitrogen intermediates (ROIs and RNIs) (5–8). Tubercle bacilli demonstrate inducible responses to oxidative stresses, and several *M. tuberculosis* genes, including *katG* (catalase peroxidase), *ahpC* (alkylhydroperoxide reductase), and *sodA* and *sodC* (superoxide dismutases) have been implicated in protection from the macrophage oxidative burst (9–11). Another potential oxidative defense system possessed by *M. tuberculosis* is a thioredoxin system composed of thioredoxin (TrxA) and thioredoxin reductase (TrxB) which requires NADH as a cofactor. The reduced form of thioredoxin is a general protein disulfide reductant, which can reactivate proteins that have been oxidized by H_2O_2 (12, 13). The ability of the thioredoxin system to reduce reactive oxygen species and thereby protect the cell against oxidative stress has been established in several systems (14, 15). Other genes, not associated with resistance to oxidants, have also been implicated as bacterial virulence factors and reveal reduced bacterial counts in different stages of disease (16–18). Although reported in genetically undefined strain variants, attenuated *M. tuberculosis* mutants that survive with normal colony-forming unit (cfu) counts in animal tissues have not been extensively characterized (19).

Studies using *in vitro* stresses such as reactive oxygen intermediates (20) and studies using macrophage infection models have demonstrated that several *M. tuberculosis* σ factors are strongly induced by conditions associated with infection (21). *M. tuberculosis* SigH belongs to the extracytoplasmic function (ECF) family of alternative σ^{70} RNA polymerase subunits (22). Expression of *Mycobacterium smegmatis sigH* is induced by both heat shock and redox stress *in vitro* (23), and *M. tuberculosis sigH* expression has been shown to be up-regulated at several time points during macrophage infection (21). ECF σ factors are believed to control the expression of gene products associated with the cell envelope and/or secreted functions of bacteria. Hence, such σ factors of *M. tuberculosis* might be expected to play a role in surface antigen expression and the secretion of immunomodulatory molecules by the pathogen.

Materials and Methods

Mutant Construction. The targeted disruption strategy was based on the vector pCK0686, which contains a hygromycin-resistance cassette flanked by unique multiple cloning sites (MCS). A left flank PCR product containing 1,722 bp proximal to the *sigH* gene and a right flank PCR product containing 2,059 bp distal to the *sigH* gene were cloned into the MCSs. The *sigH* specific flanks were nonoverlapping so that a central region of the *sigH* gene was deleted from the targeting vector, leaving 82 bp of the 5′ end and 113 bp of the 3′ end of the *sigH* gene in place. The resulting plasmid pCK0708 was then used to transform *M. tuberculosis* CDC1551 in a two-step selection process using Southern blotting to confirm allelic exchange. A complemented strain of the *sigH* mutant (pCK0758) was generated by cloning a 2,862-bp *M. tuberculosis* CDC1551 genomic fragment encompassing the coding as well as regulatory region of the *sigH* gene plus the complete coding sequences of three distal genes (MT3319, MT3318, and MT3317) into an L5 phage-based integration-proficient vector for mycobacteria, pMH94 (24), and then transforming the *M. tuberculosis* Δ*sigH* mutant with this vector.

Mouse Virulence Assays. For mouse organ cfu assays, C57BL/6 mice were inoculated by the aerosol route. The liquid inoculum placed

This paper was submitted directly (Track II) to the PNAS office.

Abbreviations: cfu, colony-forming unit(s); SCID, severe combined immunodeficient; TNF-α, tumor necrosis factor α.

‡To whom reprint requests should be addressed. E-mail: wbishai@jhsph.edu.

www.pnas.org/cgi/doi/10.1073/pnas.102055799

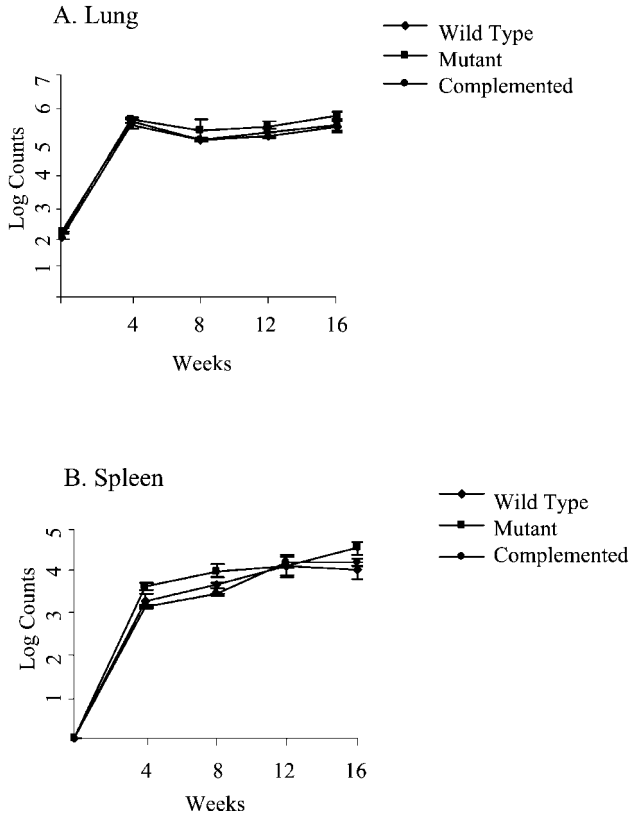

Fig. 1. Lung (*A*) and spleen (*B*) cfu counts in C57BL/6 mice infected with wild-type *M. tuberculosis* (♦), the Δ*sigH* mutant (■), and the complemented strain (●) by the aerosol route. Groups of six mice infected were evaluated at each time point.

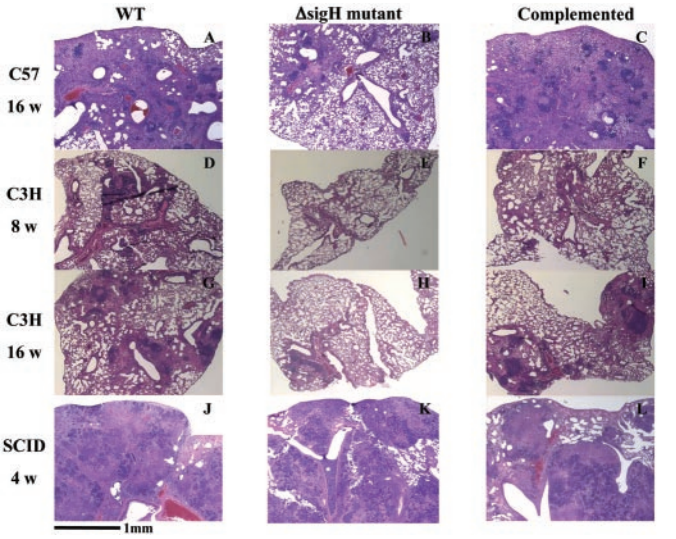

Fig. 2. The Δ*sigH* mutant (*B*, *E*, *H*, and *K*) produces less tissue pathology in lungs of infected C57BL/6 and C3H mice compared with wild-type (*A*, *D*, *G*, and *J*) and complemented strains (*C*, *F*, *I*, and *L*). C57BL/6 mice infected by the aerosol route (as in Fig. 1) were evaluated at 16 weeks (*A*–*C*). C3H mice infected intravenously with 10^6 bacilli were analyzed at 8 weeks (*D*–*F*) and 16 weeks (*G*–*I*). In contrast, SCID mice infected intravenously with 10^4 bacilli and analyzed at 4 weeks (*J*–*L*) showed no significant difference in the degree of tuberculous pneumonia. (×40; hematoxylin and eosin staining.)

in the nebulizer was determined empirically for each bacterial strain to result in the implantation of 100 bacteria per lung at day 1 of infection. Groups of six mice were killed at day 1 and weeks 4, 8, 12, and 16. Lung and spleen tissues were homogenized in their entirely in PBS/0.05% Tween 80, and colonies were enumerated on 7H10 plates grown at 37°C for 3–4 weeks. Intermediate lobes of the right lung of infected mice were saved for histologic analysis (25). For time-to-death assays C3H:HeJ and CB17-severe combined immunodeficient (CB17-SCID) mice were infected intravenously with 10^6 and 10^4 bacteria, respectively, and C57BL/6J mice were infected by the aerosol route as described above.

Fluorescence-Activated Cell Sorting (FACS) Analysis and Intracellular Cytokine (ICC) Staining. Single-cell suspensions of lung and spleen cells were prepared, washed, and plated as described (26–28) and were stimulated with anti-CD3 (0.1 μg/ml) and anti-CD28 (1 μg/ml) antibodies (Ab) in the presence of 3 μM monensin for 5 h. Cells were washed and stained with anti-CD4 (0.2 μg of anti-CD4-CyChrome Ab per 10^6 cells) and anti-CD8 (0.2 μg of anti-CD8-FITC Ab per 10^6 cells), washed, and fixed. For ICC, cells were permeabilized with saponin and stained for interferon γ (IFN-γ) (0.4 μg of anti-IFN-γ-PE Ab per 10^6 cells) or tumor necrosis factor α (TNF-α) (0.4 μg of anti-TNF-α-PE Ab per 10^6 cells) (PharMingen, San Diego) and analyzed by FACS (Becton Dickinson) as described (26–28). Cells were gated on the lymphocyte population based on cell size. Isotype controls for each Ab were used and uninfected control mice were tested in each experiment.

Microarrays. Gene-specific PCR primers were designed to amplify internal fragments from a total of 4,016 ORFs from the annotated sequences of *M. tuberculosis* CDC1551 and H37Rv (29). Individual purified PCR products were spotted in duplicate on high contact angle slides (Corning, Corning, NY) by using a 96-well format IAS arrayer (Intelligent Automation Systems, Cambridge, MA). Bacterial RNA prepared by the Trizol method was reverse transcribed and labeled with Cy3 or Cy5 probes (Amersham Pharmacia) by using the aminoallyl labeling method. The slides were scanned with an Axon Genepix scanner, and the TIGR (The Institute for Genomic Research) Spotfinder and Array Viewer software systems were used to define and quantify spot intensities. For each bacterial growth point, two independent RNA preparations from wild type and mutant were prepared, and for each RNA sample pair reverse labeling was performed (four hybridizations for each growth point). As each amplicon was spotted in duplicate, eight relative hybridization values were available for each gene for each growth point.

Results

Construction of the *sigH* Mutant and Complemented Strain. To study the role of *M. tuberculosis* SigH in the pathogenesis of tuberculosis, we used allelic exchange to delete and replace the *sigH* gene (MT3320, Rv3223c) (29) with a hygromycin-resistance gene cassette (Δ*sigH* mutant) in *M. tuberculosis* strain CDC1551 (wild type) (30). We also complemented the *sigH* mutation by cloning a complete copy of the *sigH* gene and its promoter into the single-copy integrating plasmid pMH94. The Δ*sigH* mutant, the complemented strain, and the wild-type strain showed identical growth rates in Middlebrook 7H9 medium (Difco) *in vitro*.

Proliferation and Survival in Mouse Tissues. We studied the ability of these three *M. tuberculosis* strains to survive in the tissues of resistant C57BL/6 mice by cfu analysis after aerosol exposure. Resistant C57BL/6 mice were selected for this analysis because they restrict the tissue proliferation of virulent *M. tuberculosis* and hence would be expected to amplify survival defects in attenuated strains. After aerosol exposure using inocula that implanted 100 bacilli in the lungs (as assessed by cfu counts the day after infection), mice were monitored for 16 weeks. As may be seen in Fig. 1 *A* and *B*, the pattern of mouse organ burden of *M. tuberculosis* seen with infection by the wild-type, Δ*sigH* mutant, and complemented strains did not differ. All three strains proliferated in lungs and spleen for

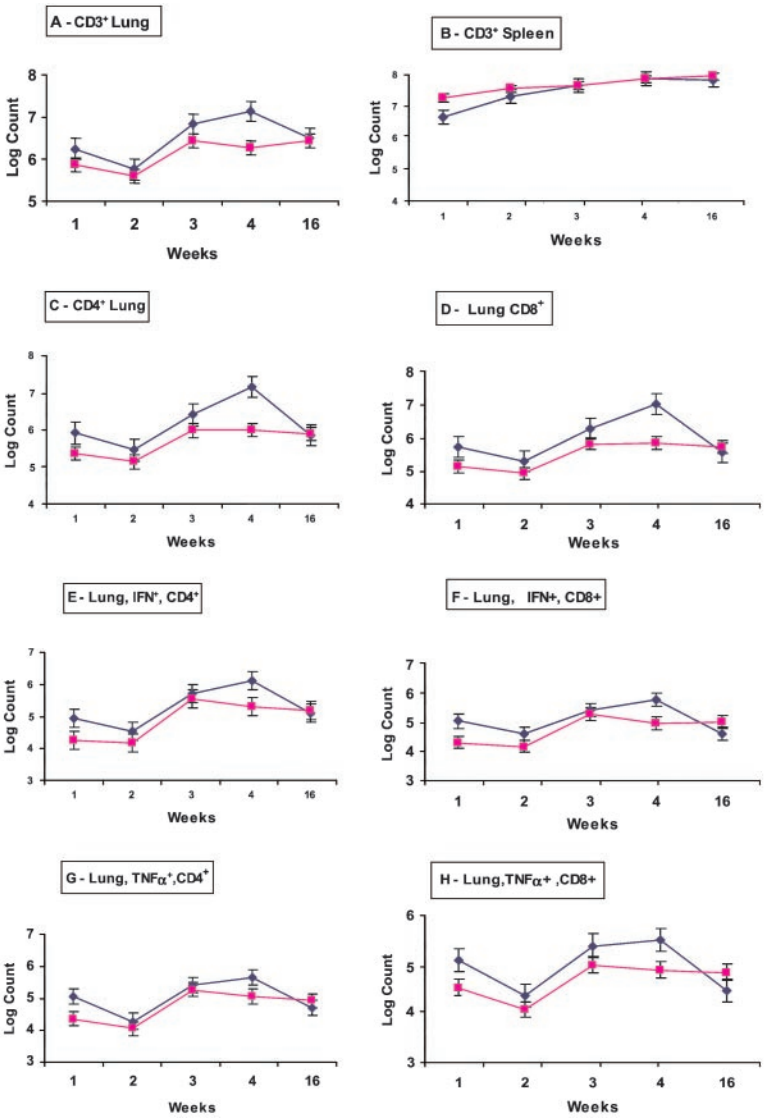

Fig. 3. Flow cytometry of cell populations from the tissues of C57BL/6 mice infected with wild-type *M. tuberculosis* (♦) and the Δ*sigH* mutant (■) by the aerosol route. Each time point represents the mean cell count from a group of four mice. Absolute numbers of $CD3^+$ cells from lungs (*A*) and spleens (*B*), and absolute numbers of lung $CD4^+$ (*C*) and $CD8^+$ (*D*) cells are shown. Intracellular cytokine staining for IFN-γ-positive $CD4^+$ (*E*) and $CD8^+$ (*F*) cells and for TNF-α-positive $CD4^+$ (*G*) and $CD8^+$ (*H*) cells from the lungs is also shown. Error bars represent one standard error.

4 weeks, and then persisted in both tissues between 4 and 16 weeks with approximately 10^6 organisms in the lungs and 10^4 bacilli in the spleen.

Histopathologic Analysis. Despite the apparent full virulence of the Δ*sigH* mutant by organ cfu analysis, histopathologic assessments of the organs from C57BL/6 mice demonstrated an attenuated phenotype in mutant-infected lungs. As may be seen in Fig. 2 *A–C*, whereas the wild-type and complemented-mutant strains produced progressive granulomatous inflammation and loss of functional alveoli attributable to enlarging and coalescing lesions, the mutant infection showed smaller, less abundant granulomas, and these lesions progressed less rapidly. After 16 weeks, mouse lungs infected by the Δ*sigH* mutant revealed minimal interstitial mononuclear cell infiltrates and peribronchial inflammation without large inflammatory wedges or granulomatous lesions (Fig. 2*B*) that were clearly observed in the corresponding wild-type and complemented strain infections (Fig. 2 *A* and *C*). A similar decrease in intensity of granulomatous inflammation and a delay in its evolution was observed in the lungs of C3H mice infected with the Δ*sigH* mutant for 8 or 16 weeks (Fig. 2 *E* and *H*) in comparison with infections by the wild-type and complemented strains (Fig. 2 *D* and *F*, and *G* and *I*). In contrast, the lungs of SCID mice infected with the three different *M. tuberculosis* strains did not show histopathologic differences at 4 weeks (Fig. 2 *J–L*), indicating that intact cellular immunity is required for the differential effect. Interestingly, analysis of spleens of all three strains of mice (C57BL/6, C3H, and SCID) indicated a similar extent of granuloma formation and tissue damage with mutant and wild-type bacterial strains (data not shown), suggesting that the disease delay phenotype in the Δ*sigH* mutant may be lung specific.

Cellular Immune Responses in Mouse Infections. We postulated that the despite the normal bacterial survival in lung tissue, the Δ*sigH* mutant lacked virulence factors that induce tissue-damaging cell-mediated immune responses by the host (31, 32). Therefore we evaluated T cell responses in C57BL/6 mice after infection by both the wild type and the Δ*sigH* mutant by using flow cytometry of cellular suspensions obtained from mouse tissues at various times after infection. As may be seen (Fig. 3 *A* and *B*), between 3 and 4

weeks, the recruitment of $CD3^+$ cells to the lung increased in wild-type-infected lungs, but not in mutant-infected mice. The reduced T cell recruitment to the lungs at 4 weeks by the Δ*sigH* mutant was observed in both total $CD4^+$ and $CD8^+$ cells with approximately one-$\log_{10}$ differences in both cell types (Fig. 3 *C* and *D*). By 16 weeks, levels of both $CD4^+$ and $CD8^+$ cells declined in the lungs of wild-type-infected mice but remained constant in mutant-infected mice, resulting in similar numbers of both T cell types. Intracellular cytokine staining for IFN-γ and TNF-α synthesis within pulmonary $CD4^+$ and $CD8^+$ cells showed that the cell-associated cytokine synthesis paralleled the T cell population curves (reduced IFN-γ and TNF-α positivity in mutant infection at 4 weeks) indicating similar rates of expression of these cytokines per cell in infection with both strains of bacteria (Fig. 3 *E–H*). By 16 weeks the levels of cytokine-producing $CD4^+$ and CD8+ cells in the two types of infection had essentially re-equalized. Thus the recruitment of cytokine-producing $CD4^+$ and $CD8^+$ cells to the lungs (but not the spleens) of Δ*sigH* mutant-infected mice was significantly blunted beginning at 4 weeks after infection. Thus the pathologic disease delay phenotype seen in lungs of C57BL/6 mice after Δ*sigH* mutant infection correlates with diminished T cell recruitment to the lung despite a bacterial burden equivalent to that of wild type.

Time-to-Death Analyses. We performed time-to-death experiments to determine whether the milder immunopathology observed in Δ*sigH* mutant infection might manifest as a prolongation of survival. When C57BL/6 mice infected with each of the three strains were held long term for time-to-death analysis, no deaths were observed in any of the three groups for 15 months in keeping with the known innate resistance of this mouse strain to tuberculosis. However, in C3H mice the Δ*sigH* mutant displayed a pronounced attenuation in time-to-death with the median time-to-death (MTD) for the Δ*sigH* mutant exceeding 170 days (0/12 mice dead at day 170) as compared with 52 and 51.5 days for infection by the wild-type and complemented strains, respectively (Fig. 4*A*, $P < 0.001$ for mutant compared with both other strains). The differences in MTD between wild-type and complemented strains in C3H mice were not statistically significant. SCID mice infected with the Δ*sigH* mutant, the wild type, and the complemented strain showed no significant difference in mortality with MTD of 32, 30, and 29 days, respectively (Fig. 4*B*, $P > 0.05$ for all pairwise comparisons).

Microarray Identification of SigH-Regulated Genes. We studied the global expression patterns of the *M. tuberculosis* Δ*sigH* mutant by using complete genomic microarrays (33–36). Total RNA from the *M. tuberculosis* Δ*sigH* mutant and wild-type CDC1551 was prepared from cultures grown in 7H9 medium to OD_{600} values of 0.3, 0.6, 1.2, and >2.0. In late exponential phase of *in vitro* growth ($OD_{600} = 1.2$) approximately 120 genes were underexpressed and 60 genes were overexpressed in the *M. tuberculosis* Δ*sigH* mutant relative to the wild type (Table 1 and Table 2, which is published as supporting information on the PNAS web site, www.pnas.org). Genes encoding hypothetical unknown proteins accounted for 30% of differentially expressed transcripts.

Several components of the thioredoxin–thioredoxin reductase system demonstrated a relative decrease in expression in the Δ*sigH* mutant by microarray analysis; these include MT4032–4033 (thioredoxin reductase and thioredoxin, repressed 3.9-fold), MT1516–1517 (thioredoxins, repressed 3.8-fold), and MT0838 (a putative thioredoxin, repressed 3.2-fold). In addition, related oxidative stress response proteins MT2541 (glutaredoxin-like, repressed 3.4-fold) and MT2063 (ferredoxin, repressed 3.1-fold) showed significantly decreased relative expression in the Δ*sigH* mutant. Several other types of stress-response genes, including MT0265 (hsp20 family member, 3.5-fold repressed), the heat-shock gene *dnaK* (MT0365, hsp70 family members, 2.9-fold repressed), MT2052, MT2061, MT2698, and MT2699 (each universal stress protein family members, repressed 2.1-, 2.2-, 4.5-, and 2.5-fold, respectively), were relatively underexpressed in the Δ*sigH* mutant. Since thioredoxins and heat shock proteins reduce and refold proteins damaged by oxidation, their σ factor dependent expression may represent a stress-management strategy by the pathogen aimed at maintaining activity of essential proteins (37). Microarray analysis of *N*,*N*,*N*′,*N*′-tetramethylazodicarboxamide (diamide)-treated strains for the most part intensified gene expression differences between mutant and wild type (data not shown), as would be expected because diamide is a known thiol-oxidizing agent.

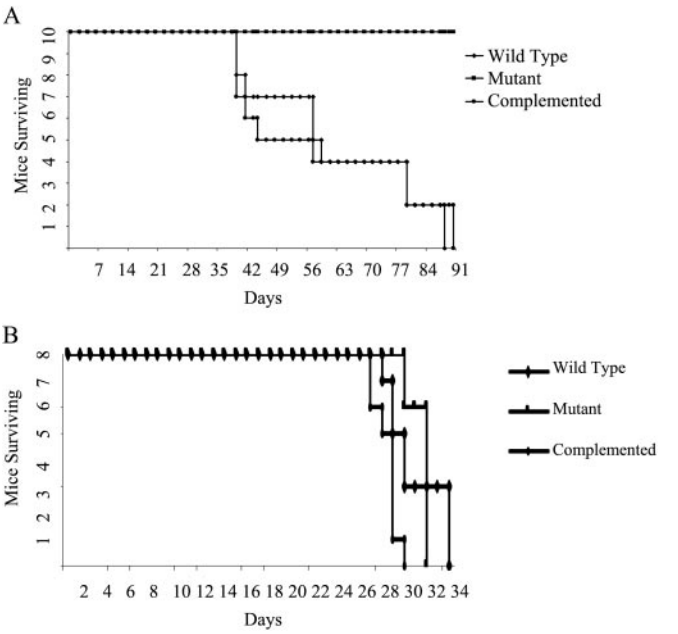

Fig. 4. Time-to-death analysis in C3H:HeJ (*A*) and SCID (*B*) mice upon intravenous. infection with *M. tuberculosis* wild-type strain (♦), the Δ*sigH* mutant (■), and the strain with complemented *sigH* gene (●) shows a significant mortality delay. The inoculum was 10^6 cfu for C3H mice ($n = 10$) and 10^4 cfu for SCID mice ($n = 8$).

Because there is a 68-bp overlap between the *sigH* gene remnant in the *M. tuberculosis* Δ*sigH* mutant and the *sigH* amplicon spotted on our microarray, it is possible to detect the level of ineffective *sigH* transcription in the mutant by microarray analysis. Rather than producing a compensatory increase of ineffective *sigH* transcription, lack of functional SigH protein resulted in a relative decrease in *sigH* (MT3320) transcription in the mutant by 4.9-fold. This finding suggests that the *M. tuberculosis sigH* gene is self-regulated, a hypothesis strengthened by the presence of a consensus *sigH*-binding sequence that was found in the upstream untranslated region of the *sigH* gene (Fig. 5).

The relative expression of gene MT3318 (Rv3222Ac), which is located distal to *sigH* in the same transcriptional unit and exhibits homology to the anti-σ factor gene class, was also diminished in the mutant strain (4.2-fold). The arrangement of genes at the *M. tuberculosis sigH* locus resembles that of the *Streptomyces coelicolor* A3(2) *sigR* locus (38, 39), and it has been shown that the gene adjacent to *sigR* (*rsrA*) inhibits SigR activity by functioning as SigR-sequestering anti-σ factor (40). Because MT3318 transcriptional levels parallel those of *sigH,* it appears likely that the SigH and the MT3318 gene product are produced in equimolar quantities. The expression of σ factor genes *sigE* (MT1259, 4.0-fold repressed) and *sigB* (MT2783, 3.4-fold repressed) was relatively repressed by Δ*sigH* mutation, suggesting that *sigH* may occupy a proximal position in the hierarchy of mycobacterial regulatory mechanisms.

SigH Promoter Recognition Consensus Sequence. Analysis of the untranslated regions of genes underexpressed in the *sigH* mutant

Table 1. A summary of the genes significantly* up- or down-regulated by mutation in *M. tuberculosis sigH* at four different phases of growth *in vitro*

	M. tuberculosis genes in the *sigH* mutant	
OD_{600}	Down-regulated by 2.0-fold or more	Up-regulated by 2.0-fold or more
0.3	15 genes including MT4032 (thioredoxin reductase); MT4033, MT1516, and MT1517 (thioredoxins); MT2063 (ferredoxin); MT2468 and MT2469 (sulfate ABC transporters); MT1163 (citrate synthase); MT2541 (conserved hypothetical protein containing a glutaredoxin active site); MT1872 (small basic protein); MT1377 (cysteine synthase); MT0040 (AMP-binding family protein); MT1924 (conserved hypothetical protein); MT1378 (rhomboid family protein); and MT3320 (*sigH*)	3 genes including MT2310 (transcriptional regulator); MT0941 (PE family protein); and MT3850 (hypothetical protein)
0.6	23 genes including MT3320 (*sigH*); MT1259 (*sigE*); MT2783 (*sigB*); MT4032 (thioredoxin reductase); MT4033 (thioredoxin); MT3938; MT1297 (multidrug resistance efflux protein); and MT2541 (conserved hypothetical protein containing a glutaredoxin active site)	9 genes including MT2310 (transcriptional regulator); MT0941 (PE family protein); MT2438 (hypothetical protein); MT0292 (PPE family protein); MT2050 (transcriptional regulator, *arsR* family); MT2027 (DNA-binding protein, *copG* family); MT2448 (peptide synthetase family); MT0146 (hypothetical protein); and MT0340 (P450 heme thiolate protein)
1.2	121 genes including MT3320 (*sigH*); MT1259 (*sigE*); MT2783 (*sigB*); MT4032 (thioredoxin reductase); MT4033 (thioredoxin); MT3938; MT1297 (multidrug resistance efflux protein); MT2541 (conserved hypothetical protein containing a glutaredoxin active site); and MT0397 (*clpB*)	60 genes including MT2310 (transcriptional regulator); MT0941 (PE family protein); MT2438 (hypothetical protein); MT0292 (PPE family protein); MT2050 (transcriptional regulator, *arsR* family); MT2027 (DNA-binding protein, *copG* family); MT2448 (peptide synthetase family); MT0146 (hypothetical protein); MT0340 (P450 heme thiolate protein); and MT2446 (hypothetical protein)
>2.0	164 genes including *sigH*; *sigE*; *sigB*; MT4033; MT4032; MT3938 (*tetR* transcriptional regulator); MT3555 (serine protease); MT2394 (malate oxidoreductase); MT2303 (malonyl-CoA acyl carrier protein); MT2150 (Xaa-Pro dipeptidase); MT2063 (ferredoxin); MT1896 and 1897 (urease subunits); MT1604–1606 (fumarate reductase operon); MT1516–1517 (thioredoxins); MT1297 (multidrug resistance efflux protein); MT1377 (cysteine synthase); MT1163 (citrate synthase); MT0631 (*tcrA* response regulator); MT0397 (*clpB*, ATP-binding subunit of clp protease); and MT2541 (conserved hypothetical protein containing a glutaredoxin active site)	71 genes including MT2310 (transcriptional regulator); MT0941 (PE family protein); MT2438 (hypothetical protein); MT0292 (PPE family protein); MT2050 (transcriptional regulator, *arsR* family), MT2027 (DNA-binding protein, *copG* family), MT2448 (peptide synthetase family); MT0146 (hypothetical protein); MT0340 (P450 heme thiolate protein); and MT2446 (hypothetical protein)

The complete list of genes significantly down-regulated by *M. tuberculosis sigH* mutation at OD_{600} of 1.2 is available as supporting information on the PNAS web site, www.pnas.org.

*Significant modulation was defined as a wild-type to mutant intensity ratio of $\geq$2.0 or $\leq$0.5 in at least 75% of the evaluable spots.

revealed a consensus sequence (Fig. 5) among at least 31 of these genes. These genes harboring a consensus element are likely to be under direct SigH control, whereas those genes that did not exhibit a consensus sequence may be indirectly controlled by SigH. The consensus sequence comprises two modules, CGGGRAC at the -35 region and CGTTR at the -10 region (R = A or G), both modules being separated by about 14–18 bp. This SigH consensus is in strong agreement with the consensus derived for six mycobacterial genes in a recent study by Raman *et al.* (41) and is similar to that observed for the sequence recognized by the *S. coelicolor* SigR protein (40).

Discussion

These data define a single regulatory gene and its dependent genes as effectors of virulence in *M. tuberculosis*. The SigH regulon comprises a global response system to manage oxidative and other denaturing stresses by inducing a family of thioredoxin and heat shock genes. Surprisingly, expression of *sigH* and SigH-mediated oxidative defenses appear dispensable for bacterial growth and survival in mouse tissues, yet they are required for disease induction and lethality in mice.

The virulence defect observed in the *M. tuberculosis* Δ*sigH* mutant falls in a newly appreciated phenotypic class in which there is reduced immunopathology despite normal bacterial replication and survival in host tissues. Steyn *et al.* (42) recently observed that mutation in *M. tuberculosis whiB3* produced a mutant strain with an infection phenotype (normal tissue cfu counts, but prolonged time-to-death) similar to that of the *M. tuberculosis* Δ*sigH* mutant. Interestingly, WhiB3 appears to bind to the *M. tuberculosis* principal σ factor SigA and is likely to be a posttranslational regulator of σ factor activity. The common thread of defective σ factor activity in both the *whiB3* and *sigH* mutants suggests that the ability to induce immunopathology and lethal infection requires the deployment of a regulated gene set and underscores the fact that *M. tuberculosis* possesses specific mechanisms that trigger deleterious host responses leading to accelerated and more extensive granulomatous inflammation (43).

Our data demonstrate that the reduced immunopathology phenotype in the Δ*sigH* mutant is related to reduced recruitment of both $CD4^+$ and $CD8^+$ T cells to the lungs at a time associated with the onset of acquired immune responses and control of bacterial replication. Concomitant with the reductions in $CD4^+$ and $CD8^+$ cells in the lung there were diminished populations of IFN-γ- and TNF-α-expressing T cells at the 4-week time point as well. The recruitment of T cells to the spleen was identical in the wild type and Δ*sigH* mutant, suggesting that the immunopathology defect of the mutant may be lung specific. It is interesting to note that whereas the entry of T cells to the lung at 3–4 weeks after infection is associated with control of bacterial growth (as in Fig. 1), replication of the mutant, which recruited 10-fold fewer $CD4^+$ and $CD8^+$ cells at 4 weeks, was inhibited to the same degree as wild type despite the influx of fewer T cells. This observation suggests that even modest cellular immune responses are sufficient to contain bacterial rep-

A

	Locus	Gene	putative promoter consensus	fold repression	SD
1.	MT4032*	trxB (thioredoxin red)	CGGGAAC-N17-CGTTC	3.9	0.9
2.	MT0365	dnaK (hsp70 family)	CGGGAAC-N17-CGTTA	2.9	0.3
3.	MT0397	clpB (protease subunit)	GCGGAAC-N17-CGTTG	2.2	0.4
4.	MT2541	conserved hypothetical protein	CGGCCAC-N19-CGTTG	14.7	5.4
5.	MT2783	sigB (principal sigma factor)	TGGGAAC-N17-CGTTA	2.2	0.2
6.	MT1259	sigE (ECF sigma factor)	CCTGGAC-N16-GGTTT	4.0	0.5
7.	MT3320*	*sigH* (ECF sigma factor)	CGGAAAT-N17-GGTTG	4.9	1.6
8.	MT0148	hypothetical protein	CGGGAAT-N17-TGTTG	4.1	1.5
9.	MT0242	transcrip. regulator, tetR family	TGGTGTC-N15-CTTGA	2.4	0.3
10.	MT1896*	ureG (urease, gamma subunit)	CGCGGCG-N16-CGTTG	2.2	0.2
11.	MT1516*	trx-1 (thioredoxin)	CGGGCCG-N16-CGTTA	3.8	0.9
12.	MT0272	chalcone/stilbene synthase	GGGCAAC-N16-CGTTG	4.9	0.7
13.	MT1102	conserved hypothetical	CGGGAAC-N16-CGTTG	2.9	0.5
14.	MT3938	transcriptional regulator	CGCGCAG-N16-AGTTT	2.4	0.4
15.	MT0631	DNA response regulator tcrA	CGGCGGA-N19-CGATA	4.4	1.3
16.	MT1297	Drug resistance efflux protein	CGGGCTG-N19-CGGTG	2.5	0.2
17.	MT1377	Cysteine synthase	CGGTCAC-N18-CGGTG	2.8	0.4
18.	MT1603*	Fumarate reductase	CGAGCAC-N17-CGTGA	2.8	0.7
19.	MT1872	Small basic protein	CGGTGTC-N14-CGTCG	2.9	0.5
20.	MT2063	Ferredoxin	CGGCATG-N15-CGTTT	7.9	1.2
21.	MT2150	Xaa-Pro dipeptidase	CGGGCAT-N18-CGCTC	3.0	0.2
22.	MT2303	Malonyl CoA acyl carrier protein	CGCGCAA-N14-TGTTT	2.2	0.2
23.	MT2394	Malate Oxidoreductase	CGCGACG-N16-CGGTC	2.3	0.3
24.	MT3555	Serine protease	CGGCAAA-N20-CGTCG	5.5	1.2
25.	MT3301	HesA/MoeB/ThiF family protein	CGGGGAA-N19-CGTTG	4.9	0.7
26.	MT3873	hypothetical protein	CGGTAGC-N16-CGATA	4.0	2.0
27.	MT3840	hypothetical protein	CGGGAAG-N17-GGTTC	2.5	0.5
28.	MT3590	hypothetical protein	CGCGAAT-N16-CGTTC	3.2	0.5
29.	MT3569	hypothetical protein	CGGGACA-N16-CATTA	8.0	3.3
30.	MT3465	hypothetical protein	CGGTGCC-N15-CGCTC	3.4	0.2
31.	MT1589	Damage inducible protein, P	CGGGGAC-N13-CGTTG	2.2	0.3

B.

***M.tuberculosis* consensus:** C_{87} G_{94} G_{77} G_{65} R_{74} A_{65} - C_{55} -N17-$C_{84}G_{97}$ T_{77} T_{90} R_{68}

***S.coelicolor* consensus:** N $G_{100}G_{100}G_{100}A_{100}A_{100}T_{100}$ -N17-$C_{67}G_{100}T_{100}T_{100}G_{67}$

Fig. 5. (*A*) Putative *sigH* promoter consensus elements identified in 5′ untranslated regions of 31 genes with reduced expression in the Δ*sigH* mutant, and the corresponding fold-repression values and standard deviation (SD) from bacteria grown to OD_{600} = 1.2. Asterisks indicate that genes immediately downstream from these were also repressed and are probably part of an operon. Bases matching the consensus are shaded. (*B*) A consensus promoter recognition sequence for *M. tuberculosis* SigH derived from the 31 putative promoters, and the reported *Streptomyces coelicolor* SigR consensus (based on an analysis of three promoters) shown for comparison (40). Subscripts denote the percent frequency of occurrence of each base among the 31 genes shown. R = A or G.

lication in a steady state at 4–6 weeks in the lungs and that the 10-fold greater numbers of $CD4^+$ and $CD8^+$ cells recruited by wild-type bacilli may constitute an overly exuberant cellular response that results in accelerated tissue damage and mortality.

While microarray analysis shows a role for SigH in the induction of an intracellular system of redox and stress response proteins to repair oxidative damage, SigH does not control the transcription of genes for well-characterized cell surface antigens or secreted proteins, which might explain in part its failure to elicit the typical cellular immune responses in the lung. One explanation for disease delay phenotype is that lack of SigH-mediated redox cycling may generate a higher proportion of oxidized or denatured bacterial antigens from the mutant that do not elicit tissue-damaging immune responses in the lung. Alternatively, the delay in disease progression may be independent of the mutant's impaired stress responses, but instead may be explained by diminished synthesis or release of pro-inflammatory surface antigens or secreted molecules that are SigH-dependent. In support of this notion is the fact that 30% of SigH-dependent genes are hypothetical proteins of unknown function, some of which may represent such antigens; additionally several transport proteins (MT2468–2469 sulfate ABC transporters and MT1297 efflux protein) and are controlled by SigH, suggesting diminished secretion of potentially pro-inflammatory molecules.

The unusual phenotype of the *M. tuberculosis* Δ*sigH* mutant emphasizes the importance of testing virulence by measures such as pathologic and time-to-death analysis in addition to bacterial cfu counts. The reduced immunopathology phenotype elicited by bacilli lacking a nonessential σ factor indicates that some *M. tuberculosis* pathogenesis mechanisms are independent of those required for survival within the host.

We thank Naomi Gauchet for helpful assistance. This work was supported by grants from the National Institutes of Health (AI 36973, AI 37856, AI 43843, and D43-TW00010), the National Vaccine Program Office, the Potts Foundation, and the Becton Dickinson Corp.

1. Dye, C., Scheele, S., Dolin, P., Pathania, V. & Raviglione, M. C. (1999) *J. Am. Med. Assoc.* **282,** 677–686.
2. Mitsos, L. M., Cardon, L. R., Fortin, A., Ryan, L., LaCourse, R., North, R. J. & Gros, P. (2000) *Genes Immun.* **1,** 467–477.
3. Turner, J., Frank, A. A., Brooks, J. V., Marietta, P. M. & Orme, I. M. (2001) *Immunology* **102,** 248–253.
4. Kramnik, I., Dietrich, W. F., Demant, P. & Bloom, B. R. (2000) *Proc. Natl. Acad. Sci. USA* **97,** 8560–8565.
5. Sherman, D. R., Sabo, P. J., Hickey, M. J., Arain, T. M., Mahairas, G. G., Yuan, Y., Barry, C. E., 3rd, & Stover, C. K. (1995) *Proc. Natl. Acad. Sci. USA* **92,** 6625–6629.
6. St John, G., Brot, N., Ruan, J., Erdjument-Bromage, H., Tempst, P., Weissbach, H. & Nathan, C. (2001) *Proc. Natl. Acad. Sci. USA* **98,** 9901–9906.
7. Storz, G., Tartaglia, L. A. & Ames, B. N. (1990) *Science* **248,** 189–194.
8. Deretic, V., Song, J. & Pagan-Ramos, E. (1997) *Trends Microbiol.* **5,** 367–372.
9. Manca, C., Paul, S., Barry, C. E., 3rd, Freedman, V. H. & Kaplan, G. (1999) *Infect. Immun.* **67,** 74–79.
10. Piddington, D. L., Kashkouli, A. & Buchmeier, N. A. (2000) *Infect. Immun.* **68,** 4518–4522.
11. Sherman, D. R., Mdluli, K., Hickey, M. J., Arain, T. M., Morris, S. L., Barry, C. E., 3rd, & Stover, C. K. (1996) *Science* **272,** 1641–1643.
12. Holmgren, A. (1985) *Annu. Rev. Biochem.* **54,** 237–271.
13. Holmgren, A. (1989) *J. Biol. Chem.* **264,** 13963–13966.
14. Mitsui, A., Hirakawa, T. & Yodoi, J. (1992) *Biochem. Biophys. Res. Commun.* **186,** 1220–1226.
15. Carmel-Harel, O. & Storz, G. (2000) *Annu. Rev. Microbiol.* **54,** 439–461.
16. Hondalus, M. K., Bardarov, S., Russell, R., Chan, J., Jacobs, W. R., Jr., & Bloom, B. R. (2000) *Infect. Immun.* **68,** 2888–2898.
17. McKinney, J. D., Honer zu Bentrup, K., Munoz-Elias, E. J., Miczak, A., Chen, B., Chan, W. T., Swenson, D., Sacchettini, J. C., Jacobs, W. R., Jr., & Russell, D. G. (2000) *Nature (London)* **406,** 735–738.
18. Glickman, M. S., Cox, J. S. & Jacobs, W. R., Jr. (2000) *Mol. Cell.* **5,** 717–727.
19. Dunn, P. L. & North, R. J. (1996) *J. Med. Microbiol.* **45,** 103–109.
20. Manganelli, R., Dubnau, E., Tyagi, S., Kramer, F. R. & Smith, I. (1999) *Mol. Microbiol.* **31,** 715–724.
21. Graham, J. E. & Clark-Curtiss, J. E. (1999) *Proc. Natl. Acad. Sci. USA* **96,** 11554–11559.
22. Lonetto, M. A., Brown, K. L., Rudd, K. E. & Buttner, M. J. (1994) *Proc. Natl. Acad. Sci. USA* **91,** 7573–7577.
23. Fernandes, N. D., Wu, Q. L., Kong, D., Puyang, X., Garg, S. & Husson, R. N. (1999) *J. Bacteriol.* **181,** 4266–4274.
24. Lee, M. H., Pascopella, L., Jacobs, W. R., Jr., & Hatfull, G. F. (1991) *Proc. Natl. Acad. Sci. USA* **88,** 3111–3115.
25. Rhoades, E. R., Frank, A. A. & Orme, I. M. (1997) *Tuber. Lung Dis.* **78,** 57–66.
26. Prussin, C. & Metcalfe, D. D. (1995) *J. Immunol. Methods* **188,** 117–128.
27. Serbina, N. V. & Flynn, J. L. (1999) *Infect. Immun.* **67,** 3980–3988.
28. Caruso, A. M., Serbina, N., Klein, E., Triebold, K., Bloom, B. R. & Flynn, J. L. (1999) *J. Immunol.* **162,** 5407–5416.
29. Cole, S. T., Brosch, R., Parkhill, J., Garnier, T., Churcher, C., Harris, D., Gordon, S. V., Eiglmeier, K., Gas, S., Barry, C. E., 3rd, *et al.* (1998) *Nature (London)* **393,** 537–544.
30. Valway, S. E., Sanchez, M. P., Shinnick, T. F., Orme, I., Agerton, T., Hoy, D., Jones, J. S., Westmoreland, H. & Onorato, I. M. (1998) *N. Engl. J. Med.* **338,** 633–639.
31. Orme, I. M., Miller, E. S., Roberts, A. D., Furney, S. K., Griffin, J. P., Dobos, K. M., Chi, D., Rivoire, B. & Brennan, P. J. (1992) *J. Immunol.* **148,** 189–196.
32. Flynn, J. L., Goldstein, M. M., Triebold, K. J., Koller, B. & Bloom, B. R. (1992) *Proc. Natl. Acad. Sci. USA* **89,** 12013–12017.
33. Behr, M. A., Wilson, M. A., Gill, W. P., Salamon, H., Schoolnik, G. K., Rane, S. & Small, P. M. (1999) *Science* **284,** 1520–1523.
34. Wilson, M., DeRisi, J., Kristensen, H. H., Imboden, P., Rane, S., Brown, P. O. & Schoolnik, G. K. (1999) *Proc. Natl. Acad. Sci. USA* **96,** 12833–12838.
35. Sherman, D. R., Voskuil, M., Schnappinger, D., Liao, R., Harrell, M. I. & Schoolnik, G. K. (2001) *Proc. Natl. Acad. Sci. USA* **98,** 7534–7539.
36. Manganelli, R., Voskuil, M. I., Schoolnik, G. K. & Smith, I. (2001) *Mol. Microbiol.* **41,** 423–437.
37. Motohashi, K., Watanabe, Y., Yohda, M. & Yoshida, M. (1999) *Proc. Natl. Acad. Sci. USA* **96,** 7184–7189.
38. Paget, M. S., Kang, J. G., Roe, J. H. & Buttner, M. J. (1998) *EMBO J.* **17,** 5776–5782.
39. Kang, J. G., Paget, M. S., Seok, Y. J., Hahn, M. Y., Bae, J. B., Hahn, J. S., Kleanthous, C., Buttner, M. J. & Roe, J. H. (1999) *EMBO J.* **18,** 4292–4298.
40. Paget, M. S., Bae, J. B., Hahn, M. Y., Li, W., Kleanthous, C., Roe, J. H. & Buttner, M. J. (2001) *Mol. Microbiol.* **39,** 1036–1047.
41. Raman, S., Song, T., Puyang, X., Bardarov, S., Jacobs, W. R., Jr., & Husson, R. N. (2001) *J. Bacteriol.* **183,** 6119–6125.
42. Steyn, A. J. C., Collins, D. M., Hondalus, M. K., Jacobs, W. R., Kawakami, R. P. & Bloom, B. R. (2002) *Proc. Natl. Acad. Sci. USA* **99,** 3147–3152.
43. Dannenberg, A. M., Jr. (1982) *Am. Rev. Respir. Dis.* **125,** 25–29.